not. Besides its possible participation in ocular entrainment by light, serotonin may be involved in mediating phase-shifting in two other ways: extraocular entrainment of the eye by red light (*3*) and mutual coupling of the circadian pacemakers in the two eyes (*4*). The presence of efferent optic nerve fibers (*2, 19*) and the large amount of serotonin in the optic nerve are consistent with the possibility of an extraocular source of the information on phase-shifting.

G. CORRENT

Biology Department, Rice University, Houston, Texas 77001

D. J. MCADOO

Marine Biomedical Institute, Galveston, Texas 77550

A. ESKIN*

Hopkins Marine Station, Stanford University, Pacific Grove, California 93950

References and Notes

1. J. W. Jacklet, *Science* **164**, 562 (1969).
2. A. Eskin, *Z. Vgl. Physiol.* **74**, 353 (1971).
3. G. D. Block, D. J. Hudson, M. Lickey, *J. Comp. Physiol.* **89**, 237 (1974).
4. D. J. Hudson and M. E. Lickey, *Soc. Neurosci. Abstr.* **3**, 179 (1977).
5. A. Eskin, *J. Neurobiol.* **8**, 273 (1977).
6. ———, *J. Comp. Physiol.* **80**, 353 (1972); *Soc. Neurosci. Abstr.* **3**, 176 (1977).
7. Circadian time (CT) 12 is the time of the last offset of light experienced by the intact animals.
8. The details of the experimental procedure and media have been described (*5*). Serotonin and other drugs were dissolved in BFSW with or without ascorbic acid (1 m*M*) which was added to retard oxidation of serotonin. Ascorbic acid had no effect on the circadian rhythm. Bufotenine was dissolved first in dimethyl sulfoxide (DMSO) and added to the tissue in BFSW with a final DMSO concentration of 0.01 percent. Neither this nor a ten times greater concentration of DMSO had any effect on the spontaneous activity or the rhythm from the eye. All solutions containing blocking agents were applied 20 to 30 minutes before treatment with serotonin.
9. H. M. Gerschenfeld and E. Stephani, *J. Physiol. (London)* **185**, 684 (1966); J. P. Tremblay, P. B. Woodson, W. T. Schlapfer, S. H. Barondes, *Brain Res.* **109**, 61 (1976).
10. Serotonin and dopamine were analyzed by gas chromatography–mass spectrometry selected ion monitoring (DuPont 21-491B mass spectrometer). The eyes or optic nerves were initially frozen. They were later placed in conical vials (Pearce) and [1,1,2,2-^{2}H]serotonin (2 ng per sample) and [2,2-^{2}H]dopamine (0.4 ng per sample) were added as internal standards. The samples were then dried in a vacuum centrifuge. Pentafluoropropionyl derivatives of the amines were formed directly in dried tissue samples by adding 6 μl of a 5:1 (by volume) mixture of pentafluoropropionic anhydride (Pearce) and ethyl acetate to each sample and heating the samples to 60°C for 3 hours [F. Cattabeni, S. H. Koslow, E. Costa, *Science* **178**, 166 (1972); *Adv. Biochem. Psychopharmacol.* **6**, 37 (1972)]. Comparable results for serotonin were obtained on pulverized and whole eyes. Serotonin analyses were performed on a gas chromatography column (1.8 m in length, 2 mm internal diameter) with 1 percent Dexsil 300 (Analabs) by monitoring masses 451 (unlabeled serotonin) and 454 (^{2}H-labeled serotonin) [D. J. McAdoo and R. E. Coggeshall, *J. Neurochem.* **26**, 163 (1976)]. The identity of serotonin was established by comparing the ratio of the intensities of masses 438 and 451 to the corresponding ratio in an authentic unlabeled serotonin sample [B. Holmstedt and L. Palmer, *Adv. Biochem. Psychopharmacol.* **7**, 1 (1973)]. Dopamine analyses were carried out at a column temperature of 170°C on a column (1.8 m in length, 2 mm internal diameter) containing 3 percent OV 17 (Varian) by monitoring masses 428 (unlabeled dopamine) and 430 ([^{2}H]-dopamine). There was no second peak in the mass spectrum of the pentafluoropropionyl derivative of dopamine that could be utilized to confirm the identity of dopamine at the signal intensities obtained in these analyses. Quantities of serotonin and dopamine were determined by comparing the heights of the peaks resulting from the endogenous compounds to the heights of the peaks from the corresponding internal standards.
11. B. S. Rothman, thesis, California Institute of Technology, Pasadena (1976).
12. M. W. McCaman, D. Weinreich, R. E. McCaman, *Brain Res.* **53**, 129 (1973).
13. J. M. Saavedra, M. Palkovits, M. J. Brownstein, J. Axelrod, *ibid.* **77**, 157 (1974).
14. H. M. Gerschenfeld and D. Paupardin-Tritsch, *J. Physiol. (London)* **243**, 427 (1974).
15. T. J. Carew, H. Pinsker, K. Rubinson, E. R. Kandel, *J. Neurophysiol.* **37**, 1020 (1974); D. C. Halstead and J. W. Jacklet, *Comp. Biochem. Physiol. A* **47**, 991 (1974); L. Harf, S. Arch, A. Eskin, *Brain Res.* **111**, 295 (1976); K. R. Weiss, J. L. Cohen, I. Kupferman, *J. Neurophysiol.* **41**, 181 (1978).
16. J. L. Luborsky-Moore and J. W. Jacklet, *J. Histochem. Cytochem.* **24**, 1150 (1976); *J. Ultrastruct. Res.* **60**, 235 (1977).
17. D. Weinreich, M. W. McCaman, R. E. McCaman, J. E. Vaughn, *J. Neurochem.* **20**, 969 (1973); M. J. Brownstein, J. Axelrod, G. H. Zeman, D. O. Carpenter, *Proc. Natl. Acad. Sci. U.S.A.* **71**, 4662 (1974).
18. Testosterone and estradiol cause changes in the periods and patterns of activity rhythms [E. Gwinner, *Science* **185**, 72 (1974); S. Daan, D. Damassa, C. S. Pittendrigh, E. R. Smith, *Proc. Natl. Acad. Sci. U.S.A.* **72**, 3744 (1975); L. P. Morin, K. M. Fitzgerald, I. Zucker, *Science* **196**, 305 (1977)]. Melatonin, which like serotonin is an indoleamine, shortens the period of sparrow circadian activity rhythms [F. W. Turek, J. P. McMillan, M. Menaker, *ibid.* **194**, 1441 (1976)]. Adrenocorticotropic hormone may phase-shift a rhythm from cultured hamster adrenals [R. V. Andrews, *Comp. Biochem. Physiol.* **26**, 179 (1968)].
19. J. L. Luborsky-Moore and J. W. Jacklet, *Brain Res.* **115**, 501 (1976).
20. Supported by NSF grant BNS 75-23452 to A.E., NIH grant NS 12567 to D.J.M., and NIH training grant 5T32 EY-07024-03 to G.C.
* Requests for reprints should be addressed to A.E.

15 May 1978; revised 11 July 1978

Medical Technology and Cost Containment: Two Applications of Operations Research

Abstract. *The government proposes "common sense" regulations to help contain rising health costs due to the increasing use of high-technology procedures, such as computerized tomography scanning. Two illustrations are given showing that such ad hoc regulations may have the effect of increasing costs and are certainly far from the optimum obtained by known methods of operations research.*

The delivery of increasingly sophisticated forms of medical care requires the availability of a wide range of medical specialists together with an array of diagnostic facilities and therapeutic equipment operated by skilled personnel. Since the costs in terms of personnel, equipment, and facilities to provide such care are increasing, issues of cost containment in health care have a high priority within the federal government.

The federal government has proposed health planning regulations (*1*) in an effort to contain such increasing costs. Many of these proposed regulations deal with major items of medical equipment, such as computerized tomograph (CT) scanners. Many of the proposed regulations contain specific fixed numerical guidelines that are apparently based on "common sense" rather than applications of the techniques of operations research. For example, for CT scanners, the Department of Health, Education, and Welfare (HEW) would like to see a scanner schedule at least 2500 patients or more per year (that is, 45 minutes per patient for 7½ hours per day for 250 days per year) (*1*). And HEW would like to see a machine load of 4000 patients per year before a second one could be installed (*1*).

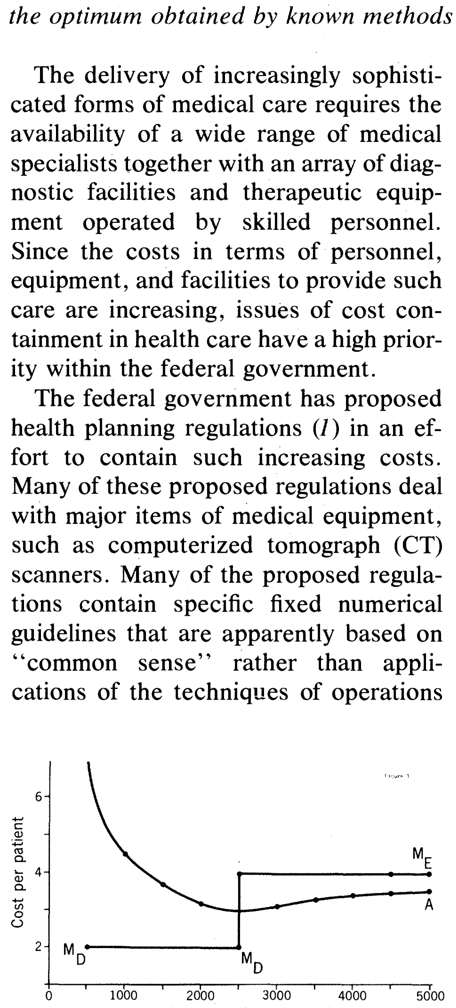

Fig. 1. Cost-output relationships under the government proposal.

As operations researchers and management scientists know, such commonsense approaches can produce far from optimum results. Furthermore, because formal methodologies and quantitative techniques have not yet been presented in conjunction with these numerical guidelines, there is no mechanism to adjust the numerical values (even if correct initially) to changing conditions and circumstances. This is especially unfortunate in high-technology areas in which local variations in patterns of utilization and rapid fluctuations in the cost of equipment and labor are the rule rather than the exception.

We have used operations research methods to show that the specific numerical guidelines in regulating major medical instrumentation can neither minimize the cost per patient nor engender cost-effective decisions. Two illustrations will be given. The first examines a guideline that assumes the cost per patient will be minimized if the number of patients per

0036-8075/78/1201-0979$00.50/0

shift is that computed for completely full utilization. However, we show that the optimum number of patients for minimum cost per patient can be substantially less than this number. This occurs primarily because of variations in patient load factors.

The second illustration examines a guideline that assumes that a specific utilization rate for a piece of medical equipment must be achieved before the purchase of a second unit is justified. We carry out a generalized quantitative analysis showing that the specification of a fixed utilization rate is rarely an optimum, but that the optimum crossover point can be calculated on the basis of the local situation and costs within the hospital in question. The two analyses presented exemplify considerations applicable to many health operations research problems involving cost containment.

We do not attempt to provide a comprehensive treatment of the myriad economic issues involved in the regulation of medical technology. Rather, we do attempt to show that the variable rates of utilization of medical technology that typify the hospital and outpatient environments must be considered when computing the least costly way to acquire and operate such equipment.

Most contemporary analyses of medical costs (*2-4*) have utilized concepts from economic theory and statistics to locate optimal utilization rates, and "break-even" points for the acquisition of new equipment. Among the most frequently used concepts (*5, 6*) are unit-cost curves showing trends in marginal costs, average variable costs, and average fixed costs as a function of the utilization rate. All of these analysts have emphasized that such analyses must be based on actual capital and operating costs at the specific site of interest. In particular, the marginal cost curve should intersect the average cost curve at the patient load where average costs are a minimum (*7*).

Figure 1 illustrates marginal cost (M) and average cost (A) curves for the government's assumption that the equipment will be completely utilized on the regular shift before it is utilized at all during overtime hours. Marginal costs remain constant as the number of patients increases to the number computed for completely full utilization (2500 patients per year). At this point, marginal costs jump as a step function to the overtime rate of operation. In this illustration the average cost curve intersects the marginal cost curve when the patient load is exactly 2500 per year.

However, in a realistic situation, the

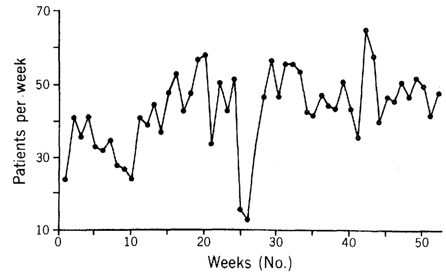

Fig. 2. Typical occupancy chart for a hospital.

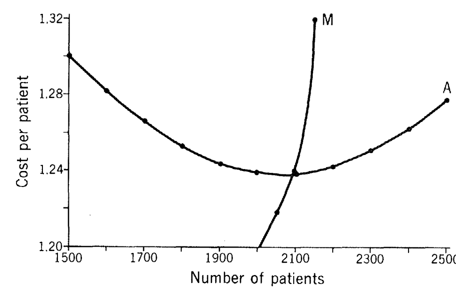

Fig. 3. Relative cost per patient (in units of cost per patient for maximum capacity of 2500); A, average cost curve; M, marginal cost curve.

patient load varies from day to day (*8*). This necessitates overtime operation on some days and first-shift idle time on other days. Also, industrial-management reports (*9*) indicate that a given work force will lose about 10 percent of its manhours because of extended sick leave, military and emergency leave, and general absenteeism. This necessitates compensatory overtime operation, and the time lost to equipment failure during the first shift further necessitates compensatory overtime operation.

A typical hospital "occupancy chart" (Fig. 2) not only applies to hospital beds utilized but also typifies load factors for major medical equipment. If the average number of patients (P) is equal to the maximum that could be scheduled during the first shift, then the equipment will have to be used at the higher overtime rate during peak loads. If the average number of patients is reduced, there will be less overtime but more idle time. If this incremental cost per patient for overtime is greater than the incremental cost per patient for the idle time, then the minimum cost per patient will be lowest at some reduction, δ, of the number of patients from P to $P - \delta$.

The annual average cost $A(\delta)$ of operating the equipment when the number of patients is $P - \delta$, including all overtime payments and other costs of extended operation, is

$$A(\delta) = \frac{F + M_d\{P - P_e[1 - f(\delta)]\delta\} + M_e\{P_e - f(\delta)\delta\}}{P - S} \qquad (1)$$

where F is the fixed costs of continued possession (such as capital depreciation), M_d is the marginal cost on the regular shift (such as supplies, wages, and benefits), M_e is the marginal cost during overtime hours (such as overtime pay and other overtime services), P is the number of patients at the maximum capacity of the equipment if used continuously during one shift per year, P_e is the number of patients that must be scanned on overtime if P patients are to be scanned during 1 year (because of the daily variation in patient load), δ is the reduction in the total number of patients from P (that is, the variable used for minimizing A), and $f(\delta)$ is the fraction of patients δ that are scanned during overtime.

It can be shown that a reasonable functional form for $f(\delta)$ is

$$f(\delta) = 1 - K\delta \qquad (2)$$

A discussion of the components of the proportionality factor K is given in (*10*).

In order to find the value of δ for which the average cost is a minimum, we take the first derivative and set it equal to zero:

$$dA/d\delta = 0 \qquad (3)$$

whence we find that

$$\delta = P - \sqrt{P^2 - \frac{P - P_e}{K} + \frac{F}{(M_e - M_d)}} \qquad (4)$$

A key variable in this analysis is the percentage of costs that are fixed as compared to the percentage of costs that vary with the number of patients. This analysis assumes that some personnel costs are variable since personnel can be assigned to other tasks if the equipment is not in use and some personnel (such as physicians) charge on a fee-for-service basis. Let us assume that

$$F = D \times M_d(P - P_e) \qquad (5)$$

that is, that the fixed cost can be computed as some constant fraction D of the variable costs during the regular shift when the number of patients for whom the equipment is used during the regular shift is equal to $P - P_e$. Let us also assume that the marginal cost of overtime operation can be represented as a multiple E of the marginal cost of regular operation (as related to the "overtime" pay rate):

$$M_e = E(M_d) \qquad (6)$$

If we assume that $D < (E - 1)$, and substitute Eqs. 5 and 6 into Eq. 4, then it can be shown that the cost per patient is a minimum when

$$\delta = P - \sqrt{P^2 - \frac{P - P_e}{K}\left[1 - \frac{D}{E - 1}\right]} \quad (7)$$

Equation 7 shows the role of the factors D, E, and P_e in calculating the number of patients for which the average cost is a minimum, where Fig. 2 characterizes the pattern of variation in load factors for the operation of a typical hospital or outpatient site. For example, if $D = 0.2$, $E = 2$, $P = 2500$, $P_e = 500$, and $K = 0.000711$, then

$$\delta = 2500 - \sqrt{6{,}250{,}000 - 2{,}250{,}000} = 2500 - 2000 = 500$$

and the optimum patient load is $2500 - 500 = 2000$.

We have run a computer simulation based on the sample of actual hospital occupancy data shown in Fig. 2. The results are given in Fig. 3, in which the marginal cost and average cost curves are shown as a function of the number of patients who utilize the equipment per year, based on $D = 0.2$ and $E = 2$. The value of 2500 is assumed for the patient capacity of the instrument operated continuously during one shift. The minimum average cost occurs near a patient load of 2100 (Fig. 3). The marginal cost curve intersects the average cost curve at the minimum average cost. A comparison of Fig. 3 with Fig. 1 shows graphically that, when variable patient load factors are considered, the minimum cost per patient occurs at a lower patient load than that computed by the government.

In order to decide when to purchase or lease a second piece of equipment, a technique must be devised to calculate the average cost as a function of the number of patients for both the single and dual equipment configurations. Griffith (*2*) and Boer (*3*) note that the marginal cost of additional service capacity will be lower than the cost of equivalent technical capacity expansion whenever the overtime and shift differential payments and other costs of extended operation are less than the equivalent annual cost of the new equipment. Capital costs can be equated to annual expenses by finding the equivalent discounted value of the investment (*11*).

In the case of the single piece of equipment, the required overtime increases with the patient load, and in the region of interest the average cost increases concurrently. In the two-machine case, the costs are greater initially because of the higher fixed costs but come down with increasing patient load because there are two regular shifts to fill before any overtime is required. Hence, the intersection of these two curves gives the desired patient load above which a second machine is cost-effective.

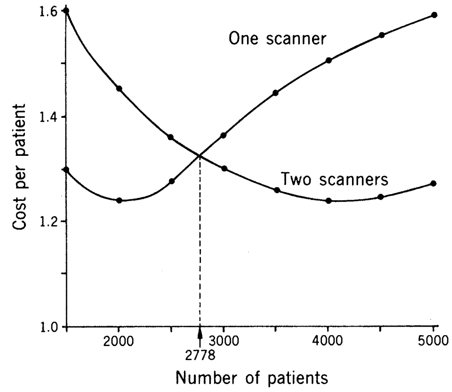

Fig. 4. Comparison of cost per patient: one scanner compared to two scanners.

The average cost for two machines is given by

$$A_2 = \frac{2F + (M_d)P}{P} \quad (8)$$

and the average cost for one machine is

$$A_1 = \frac{F + (M_d)P_0 + (M_e)(P - P_0)}{P} \quad (9)$$

where P is the number of patients that can be seen during regular time and $(P - P_0)$ is the number of patients which must be seen during overtime.

If we equate A_1 and A_2, and solve for P in terms of D and E, we obtain

$$P^* = P_0\left(1 + \frac{D}{E - 1}\right) \quad (10)$$

where P^* is the patient load at the desired crossover point or the patient load at which a second machine becomes cost-effective.

We have run a computer simulation to find the optimal crossover point when the pattern of utilization is that shown in Fig. 2, the overtime cost, M_e, is twice M_d, and the fixed costs are equal to one-fifth of the total costs per shift excluding fixed costs. Figure 4 shows the average cost curves for the cases of one unit and two units of equipment, with $P = 0.2$, $E = 2.0$, and $P = 2500$. It can be seen that the optimal crossover point is about 2800. Above this crossover point, the two-unit configuration is more cost-effective. In this example, the government's suggested patient load of 4000 patients per year is not the most cost-effective crossover point for acquiring and operating the second piece of equipment.

The results shown here apply to the cases for which D (the ratio of fixed costs to variable costs during the first full shift of operation) is less than $E - 1$ (the overtime cost rate minus one). If we assume that E is equal to two (double time), then $0 < D < 1$.

In contrast, the ratio D will be greater than $E - 1$ for situations in which the annual equivalent cost of capital equipment is greater than the annual total variable cost. Other situations in which D is large include those that require personnel so specialized that they cannot be used for other billable purposes when the machine is not in operation. In these situations, normal personnel costs must be considered fixed since they do not vary with the number of patients treated during the regular shift.

If $D > (E - 1)$, then idle time becomes at least as costly as overtime. Hence, the average cost will not reach a minimum at a patient load below the capacity of the equipment used continuously for one shift. Also, the average cost of operating two machines during the regular shift will always be equal to or greater than the average cost of operating a single machine during overtime hours. Hence, the crossover point will not occur at any patient load below the point at which it becomes necessary to operate both machines during overtime hours.

We have shown that simple operations research indicates that it is impossible to provide for all user-specific numerical values under which the cost per patient of medical technology will be minimized or at which the installation of a second piece of equipment will be cost-effective. As an alternative, quantitative procedures to assist in computing these optimal conditions as a function of site-specific parameters are presented and illustrated with computer simulations. Among these site-specific parameters are the "occupancy chart," describing variations in patterns of utilization, the proportion of regular time costs that are fixed and variable, and the overtime cost rate. The model presented does not, in itself, permit the calculation of the least costly way to acquire and operate medical technology. Rather, it illustrates the manner in which variable rates of utilization must be considered in such a calculation.

Federal guidelines for health planning regarding new medical technologies should not attempt to provide in advance specific numerical values for optimal operating conditions. Rather, they should provide analytical tools so that local health-planning agencies can calculate optimal and desirable operating conditions for facilities and equipment within their planning jurisdictions. These calculations can be updated periodically to account for shifts in labor costs, equipment costs, and patterns of utilization.

R. S. LEDLEY

T. R. THIAGARAJAN, T. P. LANDAU

Department of Physiology and Biophysics, Health Operations Research Section, Georgetown University Medical Center, Washington, D.C. 20007

References and Notes

1. U.S. Department of Health, Education, and Welfare, "National guidelines for health planning," *Fed. Regist.* **42** (No. 185), 48502 (1977).
2. J. R. Griffith, *Quantitative Techniques for Hospital Planning and Control* (Heath, Lexington, Mass., 1972), chap. 3.
3. G. B. Boer, in *Management and Cost Control Techniques for the Clinical Laboratory*, J. L. Bennington, *et al.*, Eds. (University Park Press, Baltimore, 1977), pp. 105–122.
more, 1977), pp. 105–122.
4. G. E. Louvau, in *ibid.*, pp. 123–137.
5. D. S. Watson, *Price Theory and Its Uses* (Houghton Mifflin, Boston, 1972), chap. 11.
6. G. S. Becker, *Economic Theory* (Knopf, New York, 1971), chap. 7, lecture 25.
7. In this analysis, it is assumed that the piece of equipment has already been acquired. Hence, the cost of acquisition, or "sunk" cost, is not considered as a fixed cost. Average costs are computed as the sum of the cost of continued possession of the equipment (fixed costs) and direct operating costs (variable costs). In the region of interest, regular and overtime variable costs are assumed to be linear functions of the patient load. Since the marginal costs of regular and overtime operation are computed as the derivatives of the respective variable costs, they are assumed to be constant in the region of interest.
8. J. S. Balintfy, *Proc. Inst. Manag. Sci. 6th Int. Meet.* **2**, 288 (1960).
9. O. Galbraith III and J. H. Morse, *Manage. Accounting* **54**, 42 (1972).
10. If a simplified "occupancy chart" is represented as a straight line with slope m and time period x then it can be shown that the proportionality constant $K = 1/(2x^2m)$. In reality, an occupancy chart can be described as a sequence of such straight lines. The computer simulations described in this report (see Figs. 3 and 4) are based directly on the "occupancy chart" shown in Fig. 2. No simplifying assumptions concerning the occupancy chart were made in the computations.
11. When considering the decision to acquire a second machine, costs of acquisition as well as costs of continued possession must be considered in the decision. Hence, in this analysis fixed costs (F) include both the cost of acquisition and the cost of continued possession of the machine.

4 January 1978; revised 10 May 1978

Homoeologous Chromosome Pairing: Frequency Differences in Inbred and Intraspecific Hybrid Polyploid Ferns

Abstract. *The homosporous fern* Ceratopteris thalictroides *(Parkeriaceae) has evolved a polyploid genetic system that serves to store and release genetic variability in spite of self-fertilization and Mendelian homozygosity. This is demonstrated by the segregation of a gametophyte mutant within two inbred tetraploid lines and in their intraspecific hybrid. The segregation behavior can be explained by a model involving a duplicated locus and regular homoeologous chromosome pairing. Homoeologous pairing occurs at low levels in the inbred lines and at a high level in the hybrid, indicating intraspecific differences in chromosome pairing affinities.*

Homosporous ferns are characterized by a life cycle that includes independent diploid and haploid phases. The haploid phase is represented by hermaphroditic gametophytes that produce both male and female gametes by mitotic divisions. Self-fertilization of an individual gametophyte can occur when both types of gametes are produced simultaneously. Because only mitotic divisions are involved, all gametes produced by an individual gametophyte have identical genotypes, and self-fertilization should result in the formation of completely homozygous diploid sporophytes in one generation of selfing. At the diploid level, this system appears maladaptive in that no variability, aside from mutation, can be stored or released by the genetic system of a sporophyte once selfing has occurred (*1*). It has been proposed, however, that homosporous ferns possess a polyploid genetic system in which genetic variability can be stored and released in spite of selfing (*2*). Within such a system heterozygosity is maintained within duplicated loci that are located on homoeologous (similar but not fully homologous) chromosomes. In addition, although meiotic pairing occurs preferentially between homologous chromosomes and does not result in segregation, the stored genetic variability is occasionally released when homoeologous pairing and subsequent segregation occur during meiosis (*2, 3*).

Evidence for this type of system in ferns has been primarily cytological (*4–6*). However, a study of the genus *Ceratopteris* has provided genetic evidence showing that a duplicated locus and segregation through homoeologous pairing occurs within a polyploid inbred homosporous fern (*3*). In this study, a model was formulated showing that the frequency of homoeologous pairing within a duplex heterozygote tetraploid sporophyte (for example, *AAaa*) could be determined by multiplying the frequency of double recessives (*aa*) segregating in the gametophyte generation by a factor of 4 (*7*). An additional and expanded study of this behavior, which demonstrates the presence of homoeologous pairing involving an identical duplicated locus in two inbred lines of the fern *Ceratopteris thalictroides*, is reported here. In addition, the study shows that in an intraspecific F_1 hybrid involving the two inbred lines the levels of homoeologous pairing and segregation are greatly increased.

Two inbred lines, 230Xn and 205I, of tetraploid *C. thalictroides* ($2n = 154$) were used (*8*). Both stocks were produced by selfing isolated gametophytes that were obtained from the original spore collections. Although the resulting sporophytes were complete homozygotes in a diploid sense, each inbred line segregated for pale green gametophyte mutants at low frequencies (Table 1 and Fig. 1). The pale mutant gametophytes were phenotypically identical in both lines. They grew very slowly, and frequently died under standard culture conditions on mineral nutrient medium. Pale gametophytes that reached sexual maturity on mineral nutrient medium produced pale sporophytes when selfed, but the pale sporophytes could not be grown to maturity.

The observed segregation in the gametophyte generation can be explained by assuming that the sporophytes were duplex heterozygotes (*AAaa*) for a locus affecting gametophyte pigmentation and that homoeologous pairing released the variability stored within the duplicated locus. Thus, according to the model (*3*), homozygous (*AA*) and heterozygous (*Aa*) green gametophytes and homozygous (*aa*) pale gametophytes were present in the gametophyte generations (Fig. 1). The segregation frequencies of the double recessive mutants, 1.57 percent for 230Xn and 0.67 percent for 205I, indicate levels of homoeologous pairing of 6.28 and 2.68 percent, respectively. Homozygous green gametophytes (*AA*) were presumably present at the same low frequencies, but they were phenotypically indistinguishable from the heterozygous green types.

In addition to segregating for the pale gametophyte mutant, line 230Xn also segregated for a previously reported gametophyte mutant that produced nonmotile spermatozoids (*4*). Gametophytes with nonmotile spermatozoids could not self, although they possessed functional archegonia with viable eggs. Intraspecific crosses between the two inbred lines were obtained by using swimming spermatozoids from green gametophytes of the 205I line to fertilize green, spermatozoid mutant gametophytes from the 230Xn line. The resulting intraspecific F_1 hybrids were morphologically indistinguishable from the parents, but, be-